doi:10.1017/S1431927615008752 Paper No. 0796 Microsc. Microanal. 21 (Suppl 3), 2015

Use of a hybrid silicon pixel (Medipix) detector as a STEM detector

Damien McGrouther[1], Matus Krajnak[1], Ian MacLaren[1], Dzmitry Maneuski[1], Val O'Shea[1], Peter D. Nellist[2]

[1.] SUPA School of Physics and Astronomy, University of Glasgow, Glasgow G12 8QQ, UK
[2.] Department of Materials, University of Oxford, 16 Parks Road, Oxford OX1 3PH, UK

Scanning transmission electron microscopy has traditionally relied on the high angle annular dark field technique for imaging atoms [1,2], which provides a simple and easy to understand contrast, which is strongly related to atomic number. More recently, there has been a resurgence of interest in alternative imaging modes, including bright field [3,4] and annular bright field imaging [5,6]. Ultimately, however, the most flexible STEM experiment would be to record the entire back focal plane of the specimen onto a pixelated detector, and then post-process the dataset to access whichever features in the contrast are desired. This could produce all the above-mentioned signals, but many more besides, including ptychographic reconstruction of the exit wave [7,8].

In order to achieve this aim, we need to have a detector that is capable of recording single electron events at typical beam energies for a scanning TEM (e.g. 100 or 200 keV) with enough pixels to allow significant flexibility for performing different imaging modes, a readout speed far quicker than that available of previous pixelated detectors such as traditional scintillator-CCD devices (typically < 30 frames per second), and synchronization to the scan system. We have installed a Medipix-3 detector onto our JEOL ARM200F STEM (probe-corrected, cold FEG version), which is a silicon based hybrid pixel detector with a CMOS readout architecture and 256 x 256 pixels. The Medipix family of detectors are true counting detectors. Each of the 55μmx55μm pixels contains amplifiers and digitisation circuitry that determines whether energy deposited by the incident radiation lies within the range set by user-defined low and high thresholds, counting digitally those that do. Medipix2 detectors have been investigated for TEM by us [9,10] and others [11]. Presently we are exploring the capabilities of the third generation Medipix-3 detector coupled to a high-speed read-out system. The MERLIN read-out system [12] is capable of frame rates of 1200fps for durations that are limited only by the ability to transfer frame data to non-volatile storage. Constant frame rates of 100fps are guaranteed but we have found no problems running continuously at 500fps.

Figure 1 shows that for 200keV electrons, single electron detection is achieved but the detector settings have a strong influence on the spatial frequency response of recorded images. Utilising an exposure time of 1μs and values of 70 and 240 for the pixel low energy threshold, it can be seen that the effects of charge-sharing between pixels can be drastically reduced, but at the expense of reducing the counting efficiency from 100% to ~50%. We are currently measuring the performance of the detector with respect to Detective Quantum Efficiency (DQE) and Modulation Transfer Function (MTF). An exciting aspect of the Medipix3 is its novel architecture, which allows the detection of charge-sharing and re-attribution back to a single pixel. For high-energy electrons we expect this to significantly improve MTF values.

For STEM mode detection, we have achieved synchronisation of the beam scanning and detector acquisition. Figure 2 shows a sequence of images of the bright field disc resulting from scanning across a cross-grating replica and post-processing to produce bright field (sum) and phase contrast images. This dataset was recorded with beam dwell time of 2ms and scan resolution of 256x256 pixels. The detector

operated at 500fps (total scan acquisition requiring ~130seconds) and yielded a 4-dimensional data-volume of size ~8Gb.

References:

[1] AV Crewe, J Wall and LM Welter: J. Appl. Phys. **39** (1968) p. 5861.
[2] P Hartel, H Rose and C Dinges: Ultramicroscopy **63** (1996) pp. 93–114.
[3] JM LeBeau *et al.*, Phys. Rev. B, **80** (2009) 174106.
[4] I MacLaren, *et al.*, *APL Mater.* **1** (2013) 021102.
[5] M Hammel and H Rose: Ultramicroscopy **58** (1995) pp. 403–415.
[6] S D Findlay, *et al.*, Ultramicroscopy **110** (2010) pp. 903–923.
[7] TJ Pennycook *et al.*, Ultramicroscopy (2015) *in press* (doi:10.1016/j.ultramic.2014.09.013).
[8] H Yang *et al.*, Ultramicroscopy (2015) *in press* (doi:10.1016/j.ultramic.2014.10.013)
[9] A MacRaighne, *et al.*, J. Instr. **6** (2011) C01047
[10] R Beacham, *et al.*, J. Instr. **6** (2012) C12052
[11] G McMullan *et al.*,Ultramicroscopy **107** (2007) 401
[12] R Plackett *et al.*, J. Instr. **8** (2013) C01038
[13] The authors gratefully acknowledge funding from the EPSRC under grant numbers EP/M009963/1 and EP/M010708/1. This work was supported by the EU FP7 Grant Agreement 312483 (ESTEEM2).

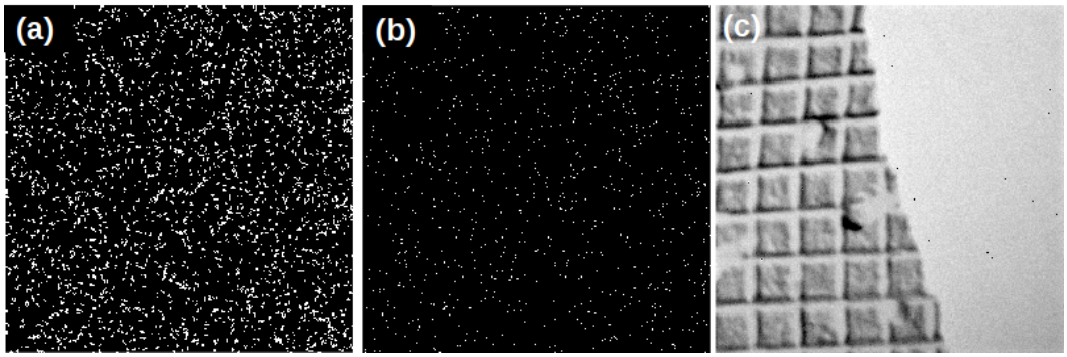

Figure 1. (a) & (b) 1ms exposures showing single 200keV electron events and charge-sharing among pixels captured with pixel low threshold values = (a) 70 and (b) 240. (c) Bright field (Low Mag mode) TEM image of a cross-grating replica (2180 lines per mm).

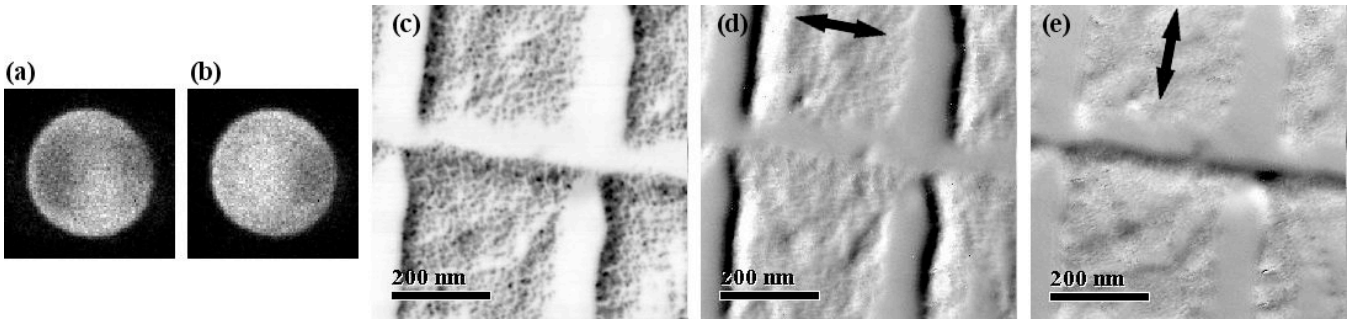

Figure 2. (a) & (b) images of the bright field STEM disc. Post-processing of the data-volume produced the STEM bright field image (c) and differential phase contrast images (d) & (e).

https://doi.org/10.1017/S1431927615008752 Published online by Cambridge University Press